Disponible en **www.hormigonyacero.com**
0439-5689 / Hormigón y Acero 2021; 72(294/295):99-116
https://doi.org/10.33586/hya.2021.3045

Structural Rehabilitation of the Old Convention Pavilion in Madrid

Rehabilitación estructural del antiguo Pabellón de Convenciones de Madrid

David Izquierdo López[a], Aurelio Domínguez[b], Maria Oslé Aizpuru[c], José Antonio Moltalvillo Fraile[d] y Luis Aznar[e]

[a] *Dr. Ingeniero de Caminos, INGEDIS, SCP. ingenieria@ingedis.es*
[b] *Dr. Arquitecto, INGEDIS, SCP.. arquitectura@ingedis.es*
[c] *Arquitecta. Subdirectora Control Edificación y Obras, Madrid Destino. Cultura, Turismo y Negocio S.A..*
[d] *Arquitecto Técnico – Ingeniero de Dirección de Ejecución Material de Obra y Coordinación de Seguridad y Salud. Madrid Destino. Cultura, Turismo y Negocio S.A.*
[e] *Ingeniero de Caminos, UTE Pabellón Convenciones (Cotodisa – Fernández Molina). laznar@cotodisa.com*

Recibido el 1 de diciembre de 2020; aceptado el 8 de junio de 2021

ABSTRACT

This article presents a detailed investigation exercise on the current state of a historical structure, including the evaluation of the state of materials and structural behaviour. The proposed partial reconstruction solution has tried to intervene as little as possible in the structure and in its current appearance, improving (as much as possible) some of the behaviours that have been shown to be ineffective or incorrect over the years.

KEYWORDS: Concrete, high – alumina cement, rheological behaviour, shell structure, historic building.

RESUMEN

Este artículo presenta un ejercicio de investigaciones detalladas sobre el estado actual de una estructura histórica, incluyendo la evaluación del estado de los materiales y el comportamiento estructural. La solución propuesta de reconstrucción parcial ha pretendido intervenir lo menos posible en la estructura y en su aspecto actual, mejorando (en lo posible) alguno de los comportamientos que se han mostrado ineficaces o incorrectos a lo largo de los años.

PALABRAS CLAVE: Hormigón, cemento aluminoso, comportamiento reológico, estructura laminar, construcción histórica.

1. INTRODUCTION AND HISTORY

The old "Convention Pavilion" or the "International Pavilion" is located in the largest public park in Madrid in the west of the city. Between the 50's and 60's, the south area of the park was developed to host the so-called "Feria del Campo", which was intended to be a biennial international exhibition, focused on the Latin-American countries centred on agricultural, cattle raising, ceramics, etc. The ground was engineered as a self – developing city with several areas and facilities, including many exhibition pavilions. One of these pavilions is the originally named International Pavilion and later Conventions Pavilion.

The Conventions Pavilion was designed in 1952 by Architects Cabrero y Ruiz [1], as a rectangular concrete sheltered structure 42 m wide by 82.5 m long. The roof is designed as a repetitive double cylindric shape shell, spanning in transversal direction, with 16 modules supported by same number of column pairs, cylindrical in shape, all in reinforced concrete (figure 1).

* Persona de contacto / *Corresponding author*:
Correo-e / *email*: ingenieria@ingedis.es (David Izquierdo)

Cómo citar este artículo: Izquierdo López, D., Domínguez, A., Oslé Aizpuru, M., Moltalvillo Fraile, J.A., Aznar, L., (2021) Structural Rehabilitation of the Old Convention Pavilion in Madrid, *Hormigón y Acero*, 72(294-295), 99-116, https://doi.org/10.33586/hya.2021.3045

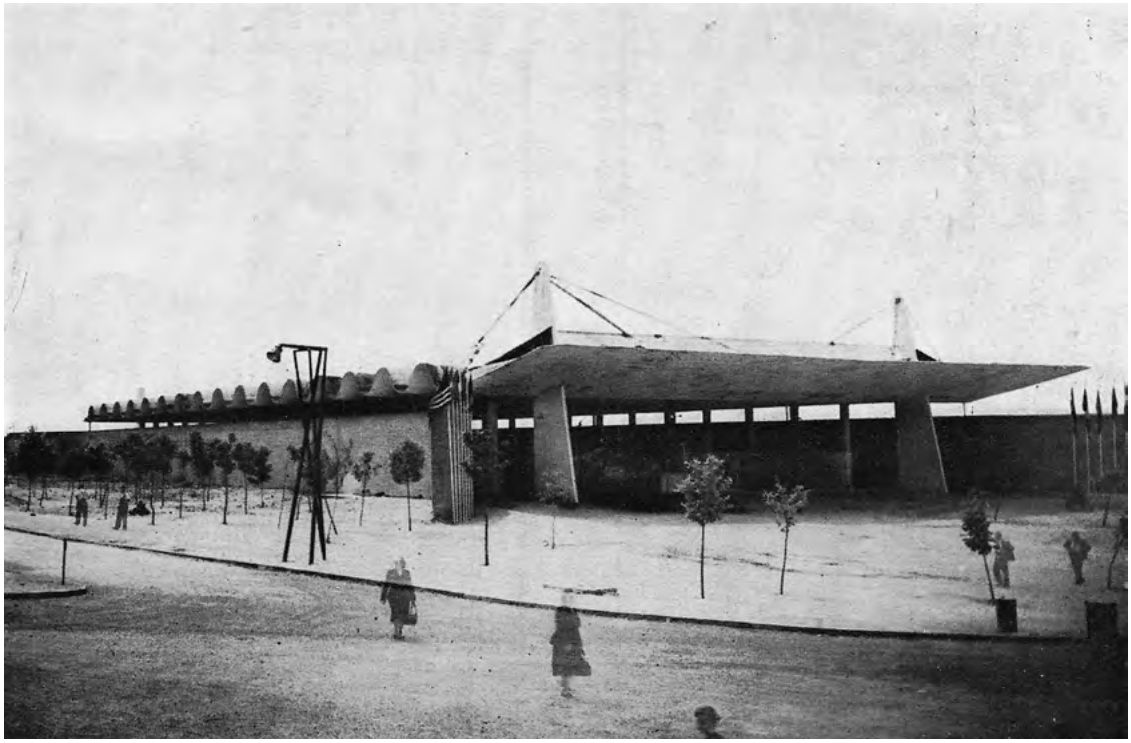

Figure 1. Original Pavilion state in 1953 [1].

Figure 2. Advertising images of the pavilion on the esmadrid website [3].

The pavilion access is starred by an emblematic canopy, guyed from two main piers with about 13 m height and walled shape, having both tapered sections. The canopy has a maximum cantilever length of 7.70 m, built in reinforced concrete. Although not confirmed, the structural design is thought to be carried out by Luis García Amorena, a well-known Architect and mathematical specialist in masonry vault analysis and design [2].

Although there is some information available in the Spanish Central Archive (A.G.A.)[1], this is limited to some architectural documents and administrative matters. One of the issues related in these documents [2] is the lack of time to finalize the erection due to a serious work delay. The resolution adopted at that time was the use of high alumina cement-based concrete in some areas of the building (at least the main piers and probably some areas of the canopy). In addition, after erecting the canopy, a great crack appeared between the last cylindric shell module, and the deep transversal beam supporting the canopy. The issue was analysed even by the great Eduardo Torroja, who assessed the structural design and confirmed its adequacy. Given the problems raised during the erection of the canopy, a symmetric structure to be located on the opposite side of the building was discarded and piers were cut, closing the rear façade with a brick wall.

During these decades, the pavilion has been used for many other exhibitions, as part of the public heritage of the Madrid City Council (figure 2). The whole building is protected as cultural heritage and its conservation is required in original shape and appearance as much as possible.

In recent years, significant increments in the main canopy deflections were observed. The problem was assessed by city technicians and, having in mind the possibility of high-alumina cement risk, the canopy was re-shored, and the building was closed. The Municipality, current structure's owner, ordered a specific structural assessment of the building and of the canopy in particular. This work was developed during 2017 in a

1 Archivo General de la Administración. Alcalá de Henares (Madrid).

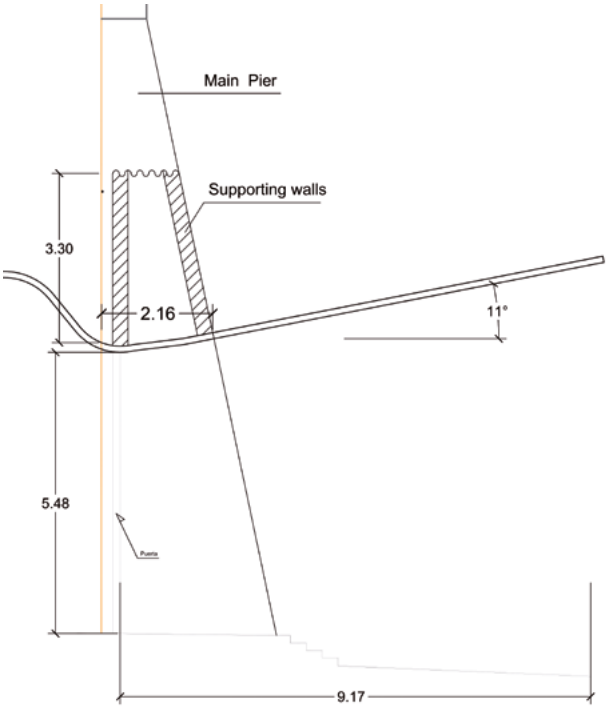

Figure 3. Existing canopy cross section and elevation.

preliminary way. The Municipality tendered the rehabilitation project, including a detailed study of the extension of high-alumina cement in the structure, as well as the reconstruction of the existing canopy, with a steel truss structure proposal. The project was awarded to a Joint Venture[2] in 2019.

2. DETAILED EXISTING STRUCTURAL DESCRIPTION AND ORIGINAL STATE

2.1. Canopy

The canopy structure has a total width of 44.14 m and cantilevers 7.60 m from the pier edges (figure 3). The canopy presents two large beams (walled shape) spanning the distance between piers (30 m) and covering the lateral cantilevers. The beams are 3.30 m in height and 30 cm thick. The concrete slab, which has a thickness of 120 mm, is supported by a grillage of concrete beams strengthened by boxed steel beams. At the beginning of the works, the canopy was fully shored with a steel structure (figure 4). There were no significant cracks or deflections noticed from the bottom face of the structure. Regarding the top face, the grillage is composed by successive transversal beams running from the front of the canopy to the wall beam at the back. These beams seem to be strengthened with additional steel profile sections or boxed plate steel sections (figure 5). In some cases, the added steel profiles are running from the centre of the canopy to the supporting piers. The stays are composed by

2 The JV was formed by Cotodisa Obras y Servicios and Fernández Molina Obras y Servicios.

Figure 4. Shoring structure for the pavilion entry canopy.

Figure 5. Canopy top face original state and stays connection detail.

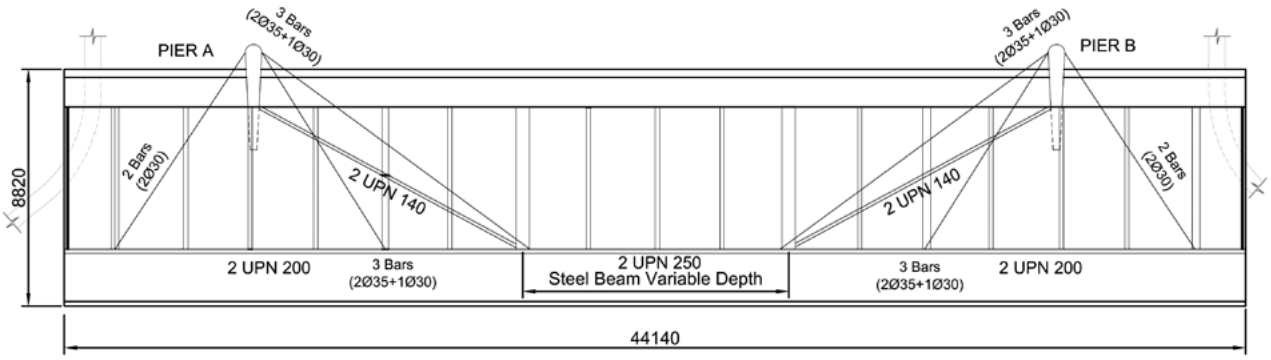

Figure 6. Plan view of existing elements in old canopy [4].

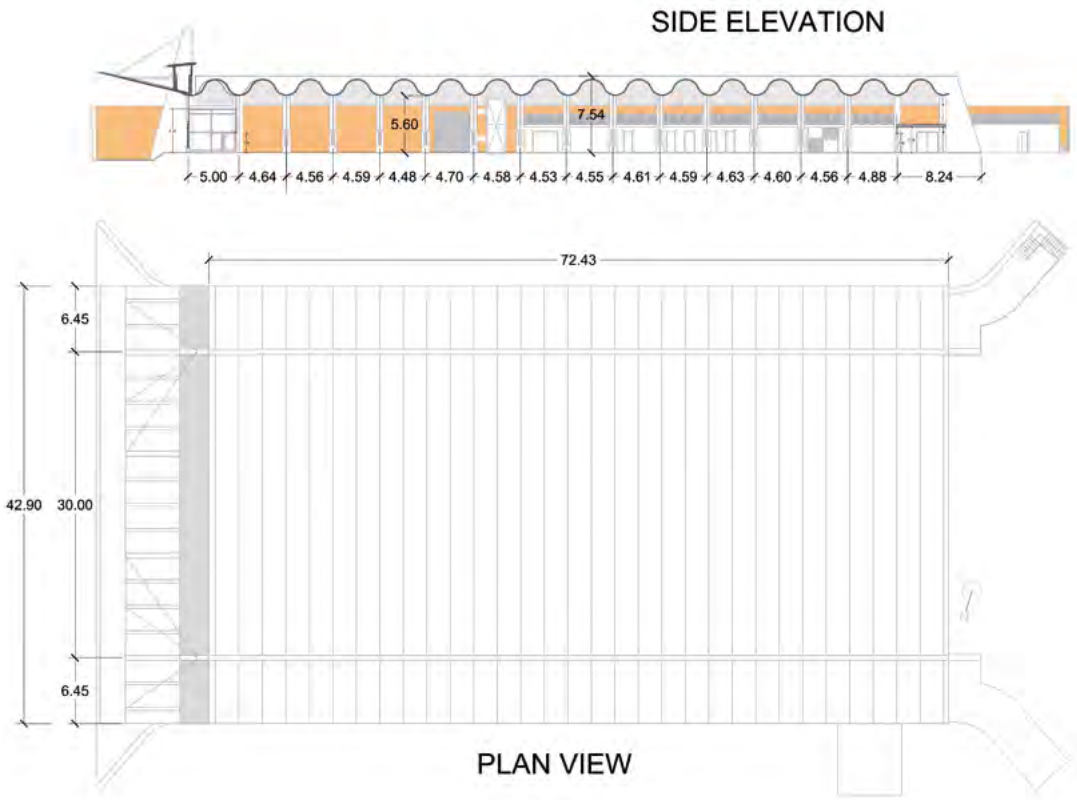

Figure 7. Plan view and elevation of roof structure.

2 or 3 ∅30 mm of mild steel bars connected to the steel beam grillage and to the pier tops. Longitudinally there is a concrete beam, approximately 2 m parallel to the edge, which is strengthen with an additional box section steel beam, with increasing depth towards the centre. Figure 6 shows a plan view of the structural elements which compose the canopy.

According to the concrete test plan developed during the first investigation campaign, high alumina cement was detected in the structure and some areas of the piers, and because of the state of the structure demolition became a necessity.

2.2. Pavilion Roof

As described previously, the pavilion roof is composed by a doubly cylindric shell structure, repeated in 16 modules each of 4.65 m width (figure 7). The shell has two lateral cantilevers of 6.45 m and a central span of 30 m, so that the moment on the centre is slightly balanced by the weight of the lateral cantilevers. The detailed shell cross section is described in figure 8. The shell has a thickness of 8 cm and a total depth of 2.00 approximately. The shell is supported transversally in a longitudinal beam of 35 cm with variable depth as per shell geometry.

Each module presents a total of six cable stays all of them composed by ∅0.5" monostrand tendons, anchored to the supporting beam, which are symmetrically disposed with respect to the module axis, see aerial view shown in figure 9. Some details of the end anchors are shown in figure 10. The beam is fully waterproofed and coated and no sign of water penetration was detected during the inspections. Detailed inspection of some strands showed that the plastic sleeve and the internal coating have provided sufficient protection to the steel, which shows no evidence of corrosion (figure 11). Given the technology of the cables it seems clear that they were installed during a strengthening work performed several years or decades after the initial erection.

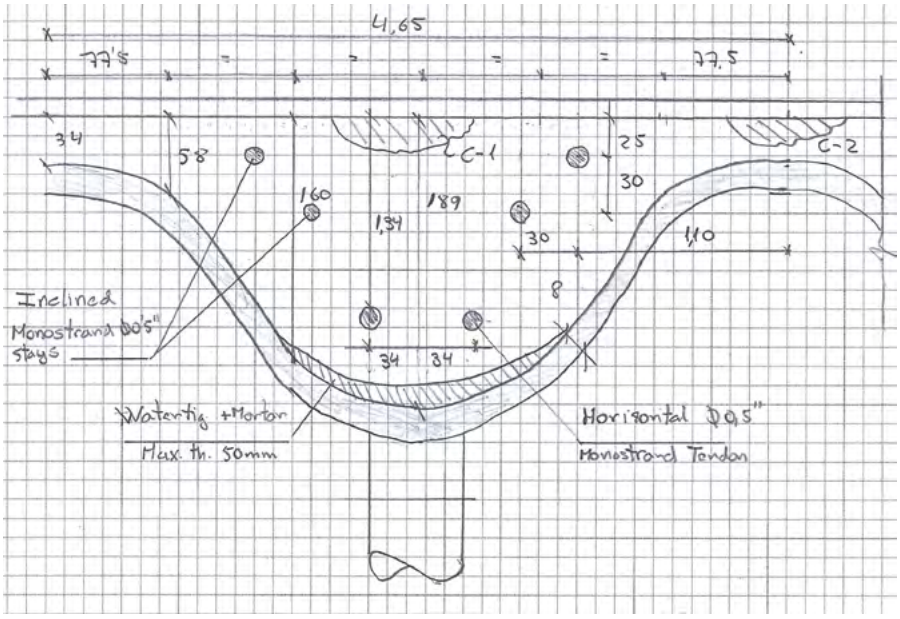

Figure 8. Detailed geometry of shell module.

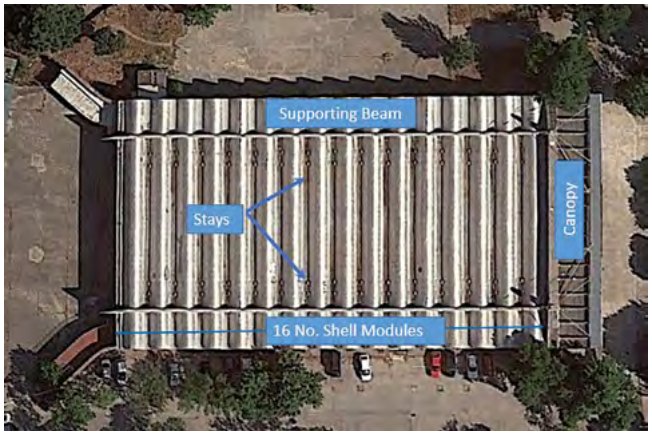

Figure 9. Aerial view of Pavilion roof. Google Earth ©.

Figure 10. Strengthening cables anchorage on supporting beam.

Regarding the shell and beam concrete material, the preliminary assessment report suggested that the shell seems to be cast with OPC[3] concrete with relatively good quality and compression strength varying from 25 to 30 MPa, whereas the supporting beams seems to be cast with high-alumina cement concrete (by appearance and colour). Preliminary core test probes showed one warning value of 8 MPa.

3. SETAILED ANALYSIS OF SUPPORTING BEAMS AND SHELL ROOF REHABILITATION

3.1. Concrete analysis and study

Once the existence of high alumina cement was confirmed by Oxine tests [5], the purpose of the study was to identify the extension of its use and the extension of the well-known crystalline transformation which yields a significant reduction of concrete compressive strength [6]. Although the Oxine tests provide valuable information regarding the existence of aluminous cement, it does not provide any information about the current amount of transformation developed or the kinetics. X-ray diffraction [7] is a more suitable alternative for investigation of the extension and potential residual strength of concrete structure with high alumina cement. However, the availability of these analyses is not as common, frequent, and fast

3 Ordinary Portland Concrete.

Figure 11. Internal aspect of strand and protective coating, the opening was made to assess the current state of the wires.

as desired. Hence a systematic study of the concrete strength of the supporting beam was developed using core test probes and ultrasound.

A total of eight tests were carried out on the aluminous cement concrete with compression strength, with varying from 19.2 to 8.3 MPa. These results show that, in those cases where the transformation is developed, a dramatic drop of concrete resistance is detected. In these areas, in situ ultrasonic pulse tests were developed in order to apply the procedure established in the EN 13791 [8] for in situ concrete strength determination. However, the ultrasonic pulse range provided in this procedure is clearly out of range for old and poor concrete quality. Thus, a simple linear correlation was adopted between measured in situ ultrasonic pulse test velocity (V) and expected concrete compression strength (figure 12).

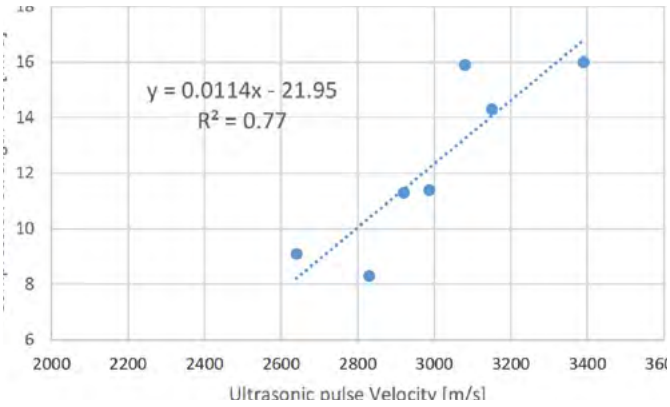

Figure 12. Estimated relationship between ultrasonic pulse velocity (m/s) and compression strength (MPa).

With an extensive mapping on the structure for pulse velocity, it was feasible to estimate the concrete compression resistance widely, ranging from a maximum of 17 MPa to a minimum of 6.5 MPa. Both values are consistent with the values obtained in core compressive strength tests performed. The statistical analysis suggests that a bimodal distribution can be fitted considering the low range as those core specimens in which the transformation is more developed whereas the upper range can be assigned to those specimens with a limited transformation. The fitted distribution is shown in figure 13, from where a characteristic value of 7.5 MPa was derived.

Although the reduction may be thought to be quite severe, it is common when dealing with aluminous cement. Figure 14 shows the compiled lower – upper bounds for the residual compression strength of high alumina cement depending on w/b (water – binder) ratio. For a concrete of the age considered, a w/b ratio of 0.6 – 0.65 can be assumed as typical. Therefore, the residual compression strength can range from 10 to 30% of its initial value.

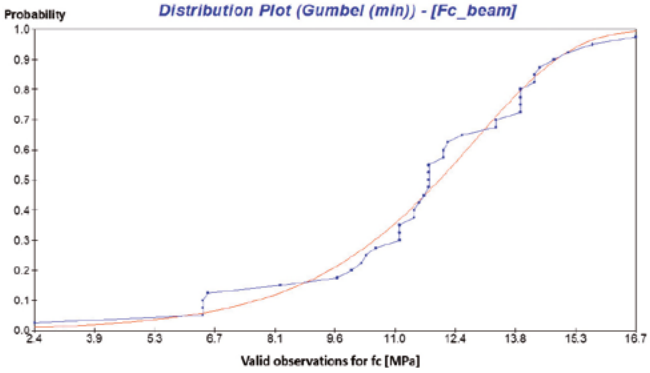

Figure 13. Statistical data and fitted distribution for estimating the characteristic value for f_c.

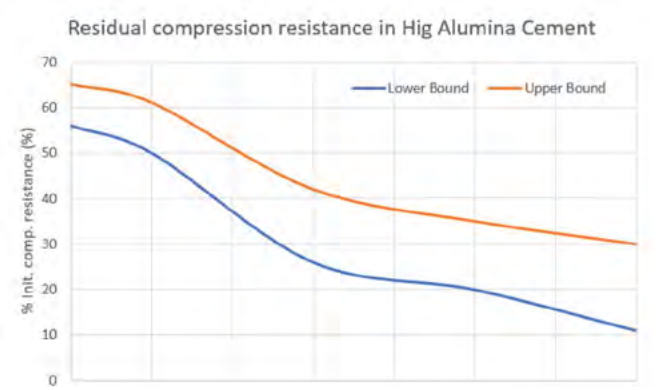

Figure 14. Residual compression resistance of concrete with Aluminous cement [6].

3.2. *Structural analysis and beam verification*

Since the structure is currently in service, even though a very low concrete strength has been identified, if the actual stresses are quite low, it might not be necessary to substitute the beams (and associated stays). Thus, a structural analysis was developed in order to assess the consequence of the poor concrete

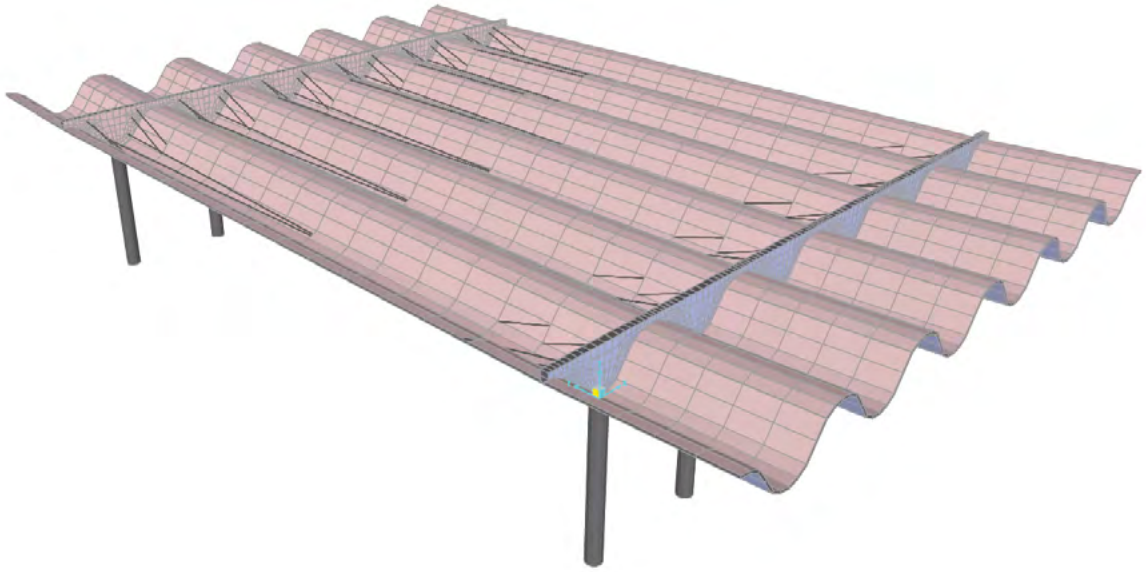

Figure 15. 3D FEM model for the pavilion roof.

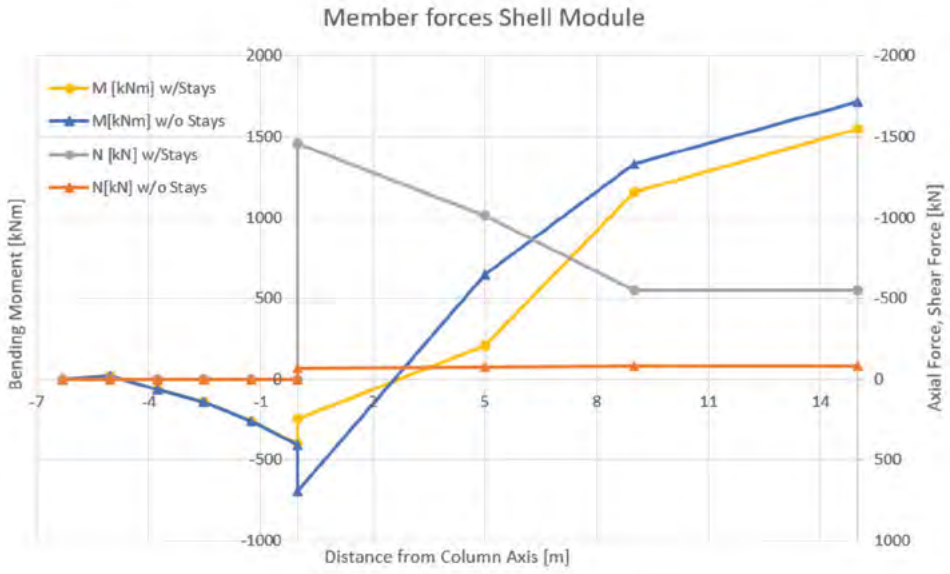

Figure 16. Estimated Original ULS shell member forces.

quality on the behaviour and safety of roof structure. For this purpose, a 3D FEM was developed including 6 shell modules together with the supporting beam, columns, and stays. The model was developed in SAP2000, given its ability to integrate the forces on elements into a comprehensive member forces to be able to postprocess with classic code equations. Figure 15 shows an image of the developed model. ULS member forces are summarized in figure 16, due to symmetry, only half of the shell structure is represented. Negative values on the x axis correspond to those sections located in the cantilever zone, whereas x = 15 m represents the midspan.

Given the reduced shell thickness, it was not easy to perform an adequate rebar survey. Only in some areas where voids exist, it was possible to identify existing rebars (figure 17). The shell cross section was verified against normal and tangential stresses, resulting in adequate safety levels, mainly due to the presence of the horizontal and inclined strands and their corresponding induced compression.

For the supporting beam, given the geometry (4.65 m span and 2.0 m deep), a D – region analysis was performed. From the 3D FEM model, the stress flow was obtained (figure 18). This behaviour was translated into a strut-and-tie model, (figure 19), considering shear forces (conservatively) hanging from the bottom of the beam. The results of this model shows that actual compression stresses in the deep beam are low enough, even for the low concrete quality observed.

However, although the obtained in-plane stresses were low enough, out-of-plane stresses (caused by the anchoring of strengthening stays) were significantly higher than allowed. It shall be noted that mobilization of these stresses is caused by induced imposed load (since the stays seems to be stressed at low level). A limitation of maintenance live loads (due to the

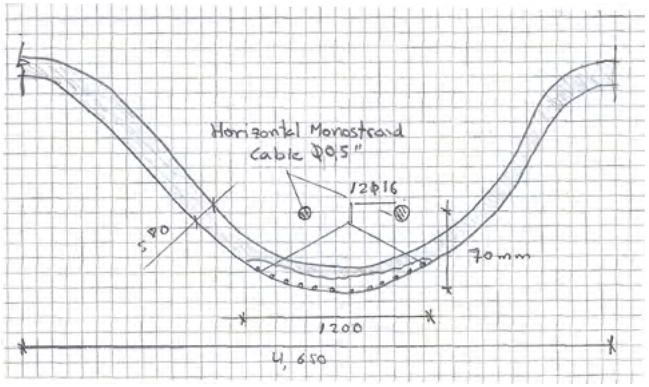

Figure 17a & b. Rebar survey from existing shell roof.

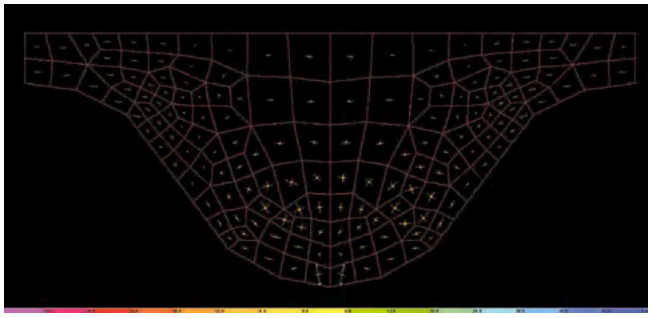

Figure 18. In-plane stress flow for the supporting beam. ELU combination.

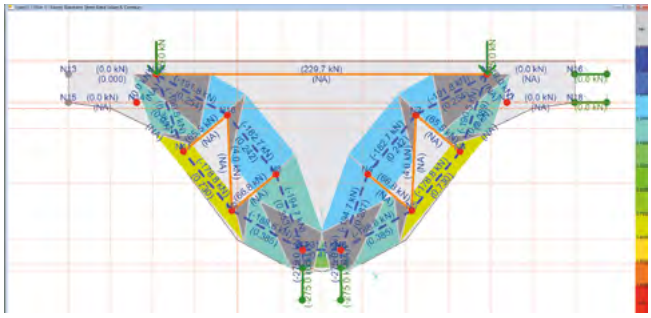

Figure 19. Associated Strut-and-tie model verification for supporting beam. In grey colour triangulation for node analysis.

pavilion closure) through the time may explain the survival of the structure despite this low concrete quality.

Failure of the stays would lead into an increase of shell member forces by more than 10% for the bending moment, and would remove the beneficial axial force, which helps the concrete section withstanding actual loads (figure 20). The load increment caused by the loss of the stays would lead to failure of the shell module in bending, requiring additional reinforcement. Thus, since external strengthening stays are essential to the structural safety, and their anchorage to the supporting beam is comprised, the main structure is in severe risk because of the low quality of concrete in the beam. Given the historical classification, the intention was to keep original design as much as possible in the strengthened condition. Hence, as final conclusion, structure owner and engineering assessment suggested, given the very low quality of concrete and the unexpected evolution of actual compression resistance (by a still developing aluminous cement transformation) to rebuild the beams keeping the geometry and using a proper concrete. The following section addresses the demolition and reconstruction works for both the beam and the existing strengthening strands.

3.3. *Supporting beam reconstruction*

As a first step, the whole structure was shored to ground (figure 21). Each module was supported on 5 steel towers, one in the middle, two additional 3 m from the columns, and two more on the cantilevers at both sides. Conservatively, the calculation of maximum reaction was based on the whole shell weight acting on the shoring and the results are shown in Table 1:

TABLE 1.
Maximum reaction for shoring structure

Shore type	1	2	3
Expected reaction [kN]	60	110	300

Figure 22 shows the location for towers. In order to control real reactions achieved in the towers, load cells were provided in one of the modules for types 2 and 3. The results are summarized in figure 23, where it is shown that actual reactions never reach more than 50% of the maximum expected value for the type 2 towers (located near columns) or 16% for type 3 (in the span centre). These results show the 3D structural behaviour of shells even without the rigid ending support. Since measurements were done three times throughout the day (early morning, midday and late afternoon), figure 23 shows some crests with daily variation, the measured midday reaction at centre of span was 30% less than the measured reaction at early morning or late afternoon. It is thought that the thermal gradient caused by sunlight (given the black colour of the shell surface) and the high flexibility of the structure, created an induced deformation in the shell that leads to unloading of the inner shoring towers, decreasing the values measured in the load cells, although no measurements were performed to confirm this hypothesis.

Demolition works started from the opposite side of the main entrance and works involved two consecutive modules at a time. In order to maintain the existing rebars, hydrojet demolition was suggested as a way to proceed. However, the low concrete quality allowed the contractor to perform adequately the works without any affection to the existing reinforcement (using more traditional demolition techniques, pneumatic

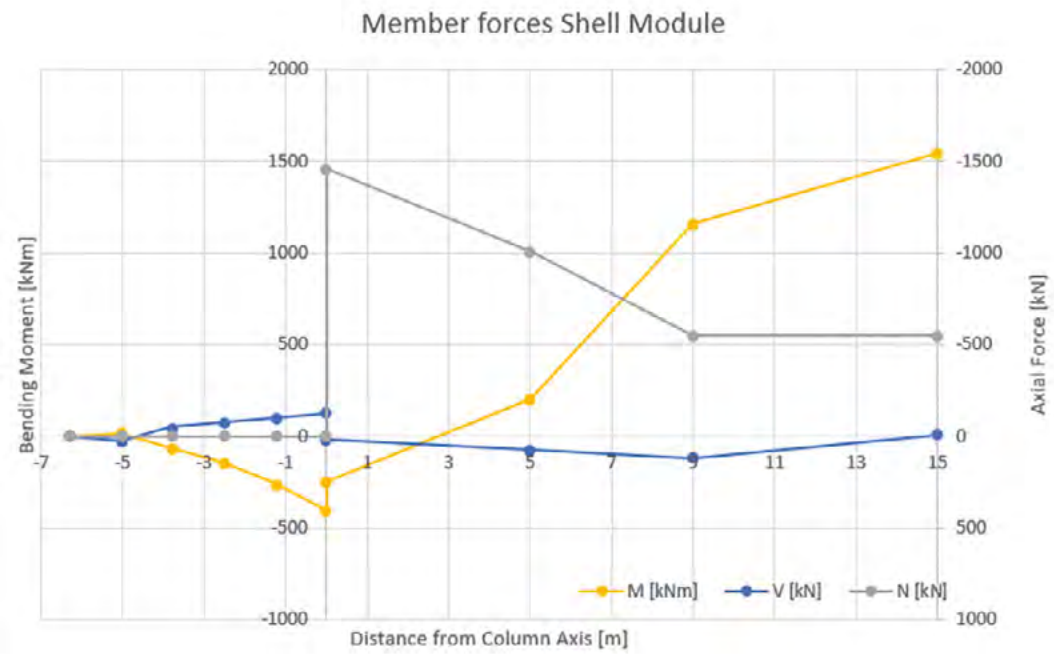

Figure 20. Comparison shell module member forces with and without (w/o) external stays.

Figure 21. Temporary shoring to ground.

hammer (figure 24). It was noticeable that although the aluminous cement concrete was of low quality, no significant signs of rebar corrosion were detected, probably due to the good waterproofing used since years in the existing beam.

Preformed movable formwork with enough stiffness was created having enough tolerance to cover the geometrical imperfections detected in the structure (in some cases with more than 5 cm). New strand alignment and concreting was made without significant problems. The whole cycle for one module took one week, completing the demolition and reconstruction of every two beams in only 10 weeks.

After concreting of all modules, new stays were provided and were prestressed in the predefined order. Existing anchor blocks of inclined stays at the top of the shell, were demolished as well, keeping the existing reinforcement (figure 25). During demolition it was detected that the existing rebars presented several difficulties to be used for strand anchoring, due to the small gap between the hairpin and shell surface, which limited the stay angle (figure 26). During prestressing, the bottom horizontal stays were stressed up to 200 kN (75% of tensile strength) without any problem. However, in the case of shorter cables, the lack of existing block reinforcement, due to the aforementioned geometrical problems, produced some anchoring blocks to fail in transmitting the force to the shell (figure 27). In those cases, the stressing force was limited to the

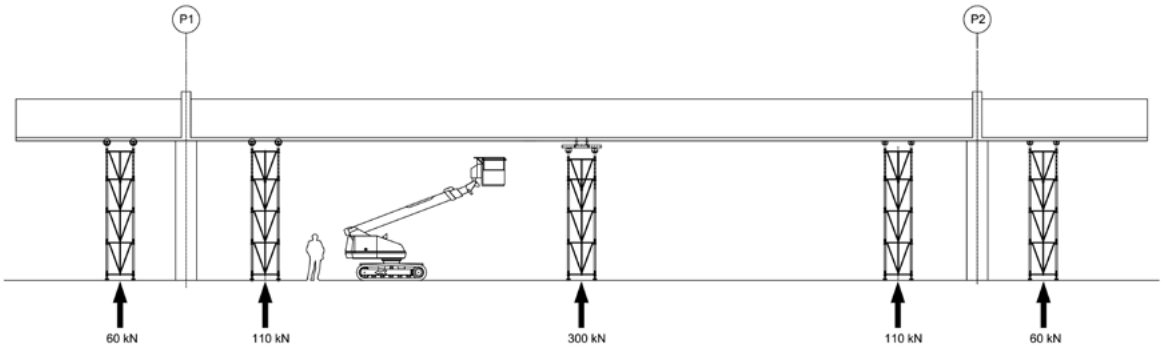

Figure 22. Temporary shoring to ground location and maximum expected reactions.

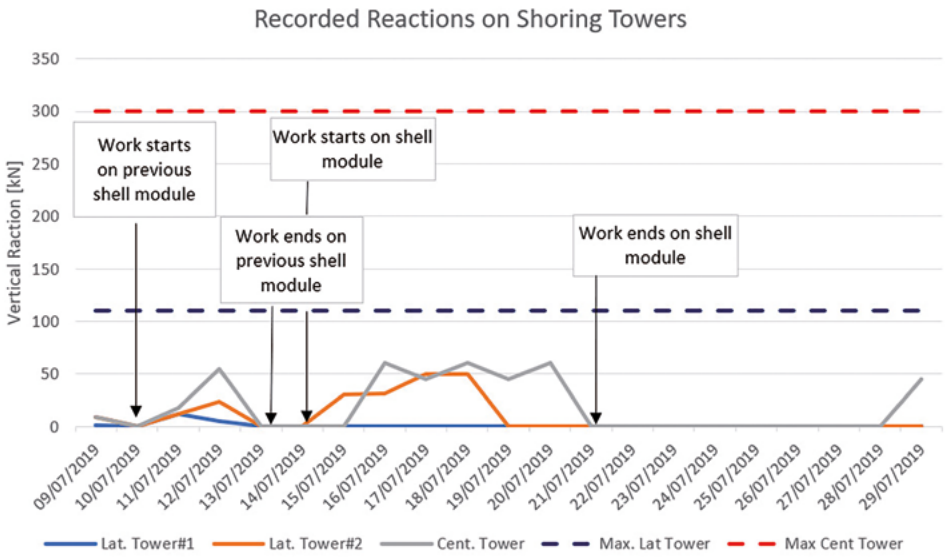

Figure 23. Registered reactions in towers vs maximum expected.

Figure 24. Supporting beam demolition and original underlying rebar configuration.

50% of tensile strength after reassessing the structure and the block was repaired by partial demolition and rebuilt. Structural verification was performed using reduced stressing force, with adequate results. Once the stressing force was reduced, the stressing procedure performed correctly and without any relevant problem. During stressing, available load cells on the steel towers measured full unloading, verifying the adequate structural behaviour as expected.

Once the beam reconstruction was finished, finishing works included roof waterproofing and coating, and the bottom face sandblasting and coating with an anticarbonation paint, trying to recover the original concrete appearance of the shell roof. All works were performed in only 16 weeks including waterproofing and coating. Figures 27 to 29 show some views of the final shell roof appearance after rehabilitation and beam reconstruction.

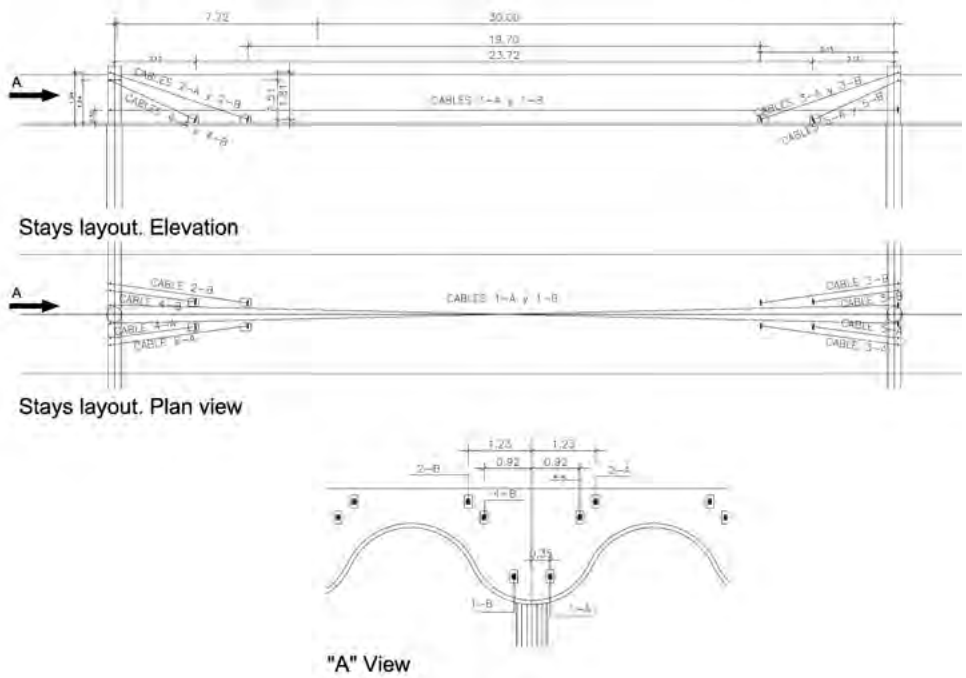

Figure 25. Definition of strengthening stays.

Figure 26. Existing reinforcement in the shell passive anchor block and anchorage failure.

Figure 27. Final state shell roof after rehabilitation.

Figure 28. Final state shell roof after rehabilitation.

Figure 29. Final state shell roof after rehabilitation.

4. DETAILED ANALYSIS OF CANOPY RECONSTRUCTION

4.1. Structural typology selection

Preliminary design proposed the substitution of the supporting walls linking both piers by a steel truss, approximately 2.60 m height and 2.0 m wide. From this truss, composite members were placed perpendicularly to the structure, supported by 4 stays from the piers and one additional stay from the truss beam.

After the complete geometrical survey of the existing structure, several inconsistences and imperfections were found, and caused the steel structure not to be compatible with required tolerances for fabrication.

The most suitable solution to this field issue is, logically, a concrete beam, which can be adapted to real geometry and imperfections. The main reason argued to discard the concrete solution during preliminary design was the imprecision in determining the deflections, especially for a given structure suffering torsion as is the case. Thus, any validation for a concrete solution should include a refined analysis of deflections in the canopy, including uncertain effects in concrete, such creep, shrinkage or cracking.

The structural behaviour of the existing canopy seems to be simple. Vertical forces are supported by transversal beams, which are hung from the stays to the pier and directly supported on the existing pair of deep beams linking the piers (figure 30). The eccentric support on the deep beams causes some degree of torsion, which is resisted by a couple of vertical forces. Longitudinally, the steel box section running parallel to the canopy edge and connecting stay ends, transfers the load to the stays, whereas the two deep beams are supported on both piers spanning the 30 m between them (figure 31). Simplified analysis suggests that forces are not so high in the deep beams

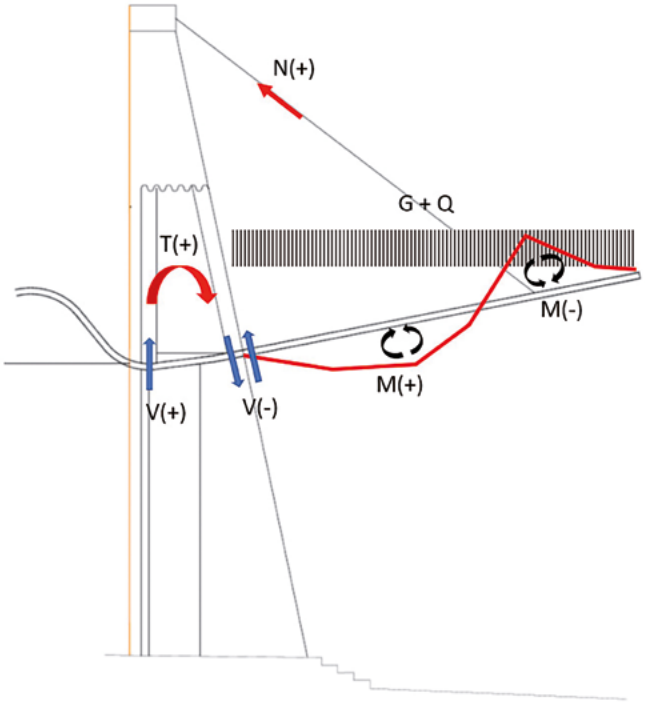

Figure 30. Simplified canopy structural behaviour (transversal scheme).

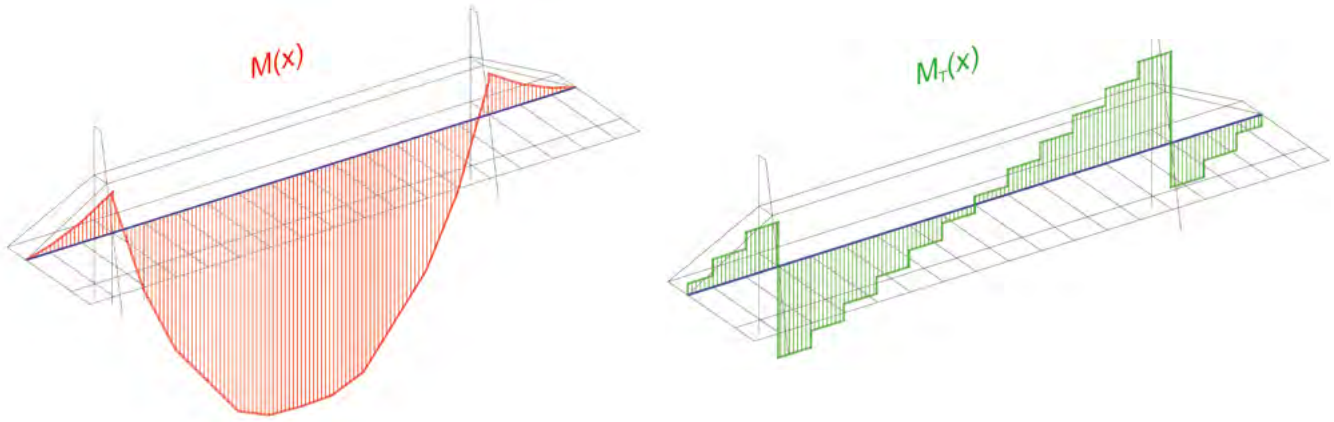

Figure 31. Simplified canopy structural behaviour (longitudinal scheme).

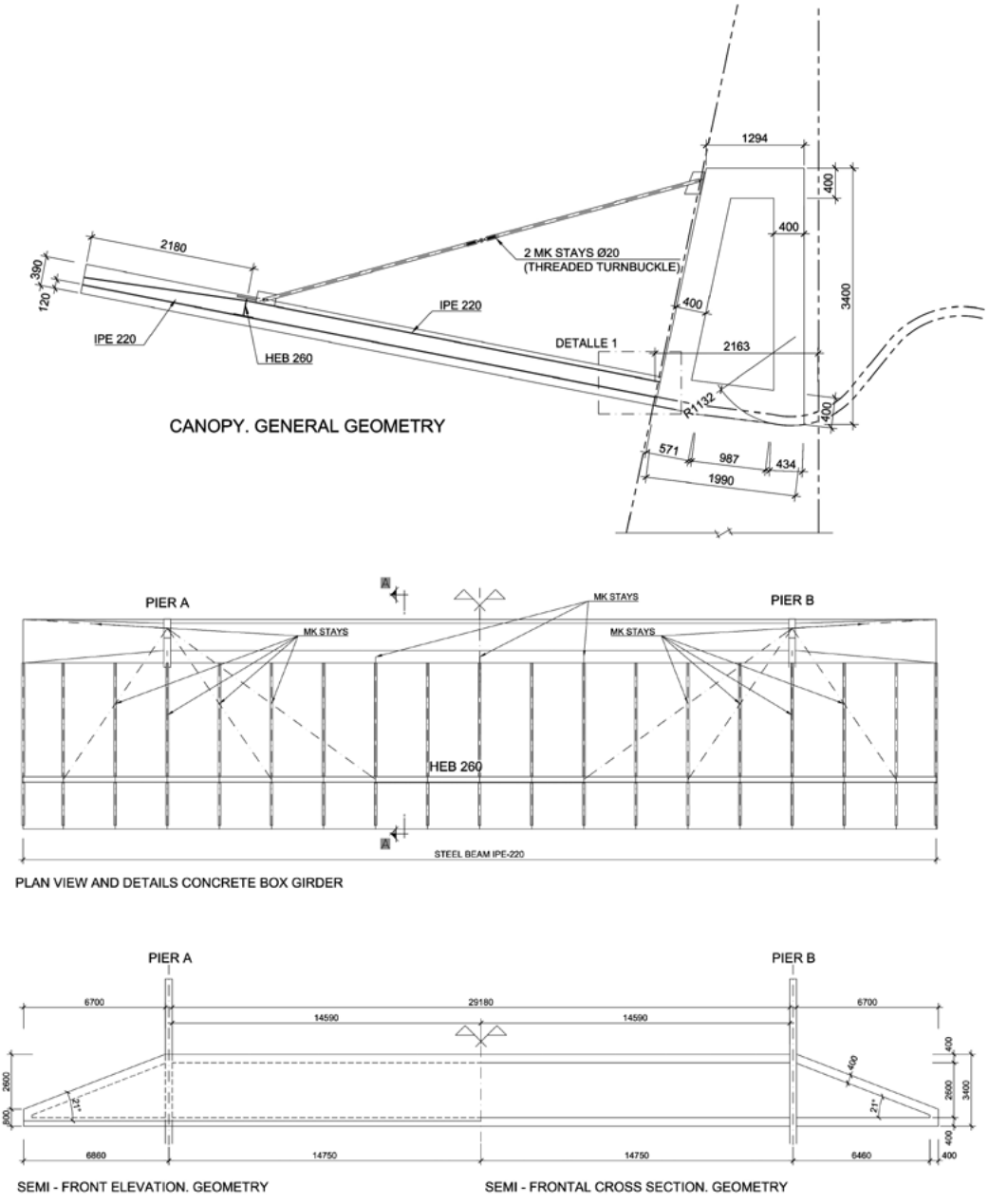

Figure 32. Proposed structural arrangement for new canopy.

nor the transverse beam to cause the severe deflection identified in the structure.

A quantitative estimation of torsional stiffness was performed, in order to assess the decision of keeping the proposed truss beam (properly adapted for the irregularity of the existing geometry) or adopting a concrete box girder. For a truss beam with 2.45 m in height and 1.60 m wide, with HEB-200 steel profile chords and diagonals, the approximate torsional stiffness can be calculated by equation (1), [9]:

$$G_s I_T = G_s 4 \frac{(b\,e)^2}{\frac{(2b+2e)^2}{t_{eq}}} \quad (1)$$

Where:

b is the width of the truss

e is the lever-arm for the truss (distance between top and bottom chord) and,

t_{eq} is an equivalent thickness given by following expression (2)

$$t_{eq} = \frac{E_s}{G_s} \frac{a\,b}{\frac{d^3}{A_d} + \frac{b^3}{A_m} + \frac{a^3}{12}\left(\frac{1}{A_s} + \frac{1}{A_i}\right)} \quad (2)$$

Where:

E_s is the steel's Young modulus

G_s is the steel's shear modulus

d is the diagonal length

A_d is the diagonal area

A_m is the upright area

A_s is the top chord area

A_i is the bottom chord area

The calculations provide a range of torsional stiffness values between 0.6·106 and 1·106 kNm^2.

For a concrete box section, having similar external dimensions and wall thickness between 30 and 50 cm (figure 32), stiffness will range between 2 and 3.5·108 kNm^2, where accounting for a reduction due to cracking of 0.3 and a creep factor of φ = 2.50 results in a a more realistic range between 1.6 and 3 107 kNm^2. These figures are about of 20 times higher than those provided by the steel structure, suggesting that the use of this alternative is more efficient that the steel solution.

For the slab solution, the preliminary proposal was that of an inverted composite floor (having a solid concrete slab at the bottom).

4.2. Detailed study of canopy deflections and forces

Having in mind the concern raised by the structure's owner regarding the structural appearance and the deflection control, a detailed structural analysis was performed, evaluating all deflections at initial and long – term, including all concrete rheological aspects.

Given the size of the box section and piers, the model was developed using shell elements. Composite sections were modelled using 1D elements, with tributary concrete area, whereas stays where modelled using also 1D elements, with

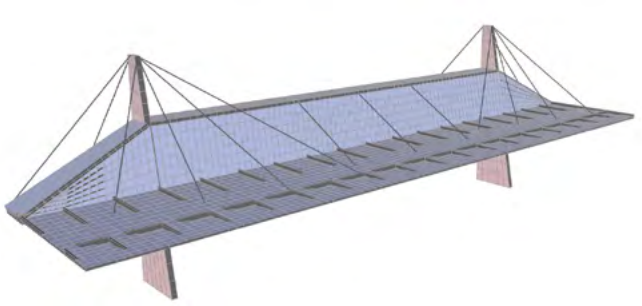

Figure 33. Canopy, 3D structural model.

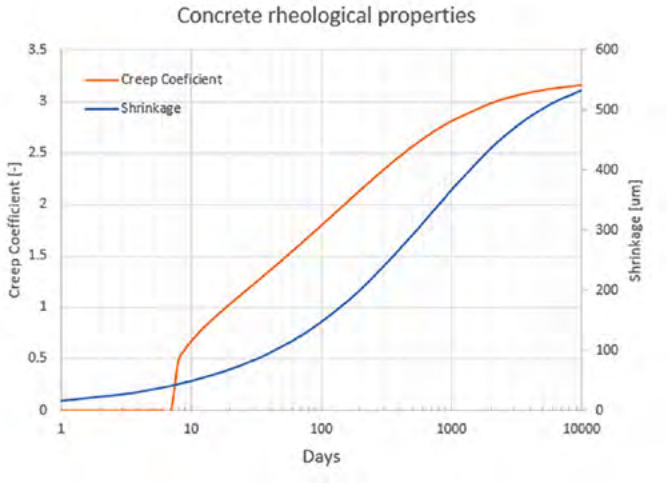

Figure 34. Creep and Shrinkage considered for the concrete.

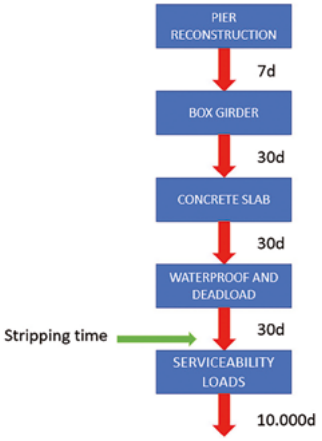

Figure 35. Construction schedule for structural analysis.

no compression capacity. Figure 33 shows the image of the 3D model developed for the analysis.

Concrete material behaviour included all time dependent properties, such as evolution of concrete strength (and associated E-modulus), shrinkage and creep. Analytical models as per EN1992-1-1:2004 [10] were used with a Class N cement type and 50% of RH. Figure 34 shows the evolution of the rheological parameters from casting to infinite time. In case of composite beams, both rheological parameters were included in the behaviour of the 1D FEM, causing local redistributions. As for any time – dependent structural analysis, an erection schedule was defined. Thus, the schedule considered in the analysis is defined in figure 35. Five steps were considered in

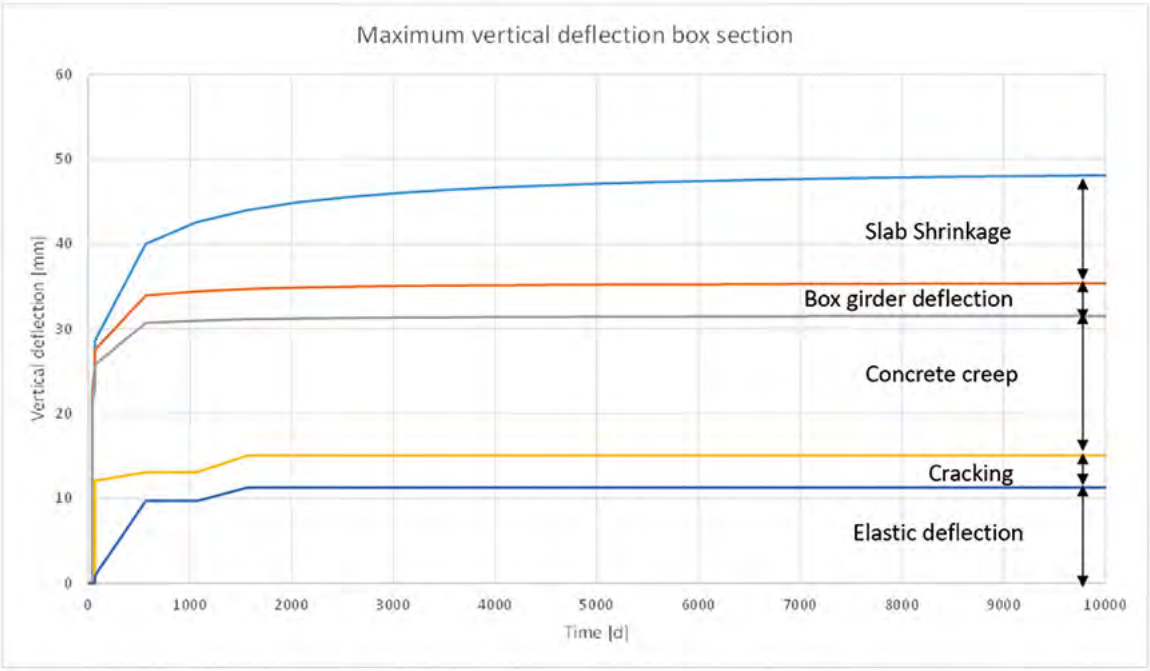

Figure 36. Effect of different actions on the calculated maximum deflection at the canopy edge for the initial solution.

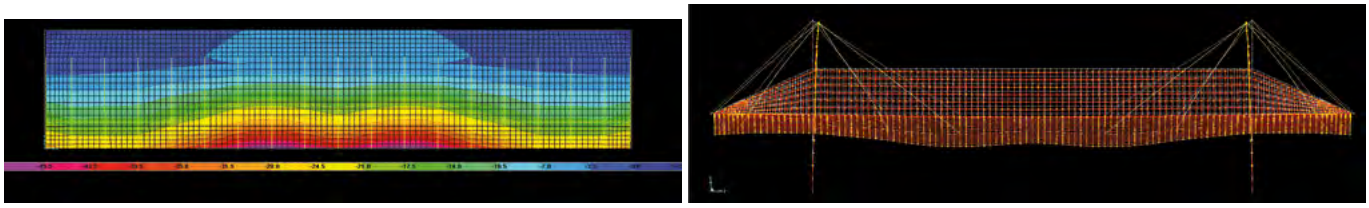

Figure 37. Final vertical deflection distribution for canopy structure for initial solution.

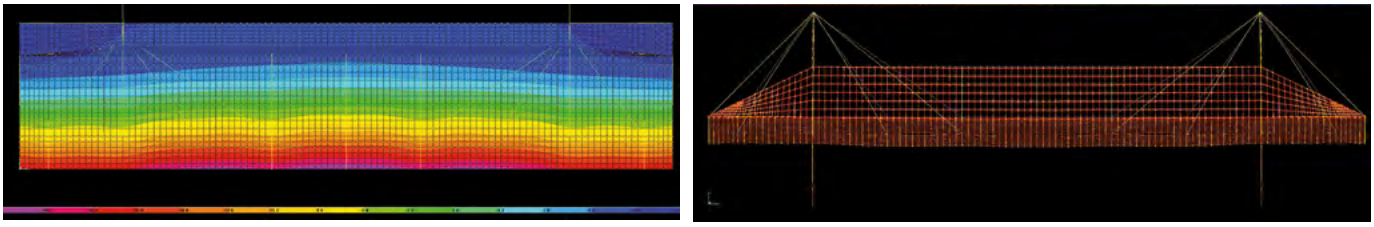

Figure 38. Final vertical deflection distribution for canopy structure for adopted solution.

the construction schedule. The works would start by pier reconstruction with OPC concrete and removing existing high alumina cement. After pier reconstruction the box girder erection will begin. Finally, the concrete slab and steel beams, working as a composite structure, will be constructed. Waterproofing and other superimposed dead load are applied after structural completion (67 days). Finally, the structure shoring is removed in 30 additional days. 10.000 d was considered as the end of time – dependent analysis.

In order to capture cracking, given the considerably complexity, an *a priori* stiffness reduction was considered in the analysis. The box section stiffness was reduced to the 70% of the theoretical value (after beam stress analysis), whereas the stiffness of the concrete slab was reduced to the 30% of its theoretical value.

The maximum calculated deflection at 10 000 days was 48 mm. In order to quantify the components that play a role in the deflection behaviour, the model was updated by removing some features: Shrinkage, Creep, Box girder deflection and stiffness reduction due to cracking. The obtained results are summarized in figure 36, together with the time evolution and show that creep and shrinkage are major contributors to the final deflection calculation (29 mm from the total 48 mm calculated), whereas other aspects such as box girder deflection or cracking are negligible (representing only 3 mm in the total cumulated deflection). Note that shrinkage plays a significant role, given the location of the concrete slab in the composite section, at bottom. Concrete shrinkage induces a positive curvature in the cantilever and increases the deflections in the canopy edge. Two lessons were derived from the analysis: first, the use of controlled shrinkage cement will lead to a relevant reduction of maximum expected deflection (- 25%) and second, the longer the shoring remains, the lower the final deflection will be.

Some additional information was extracted from the analysis of vertical deflection in the structure (figure 37):

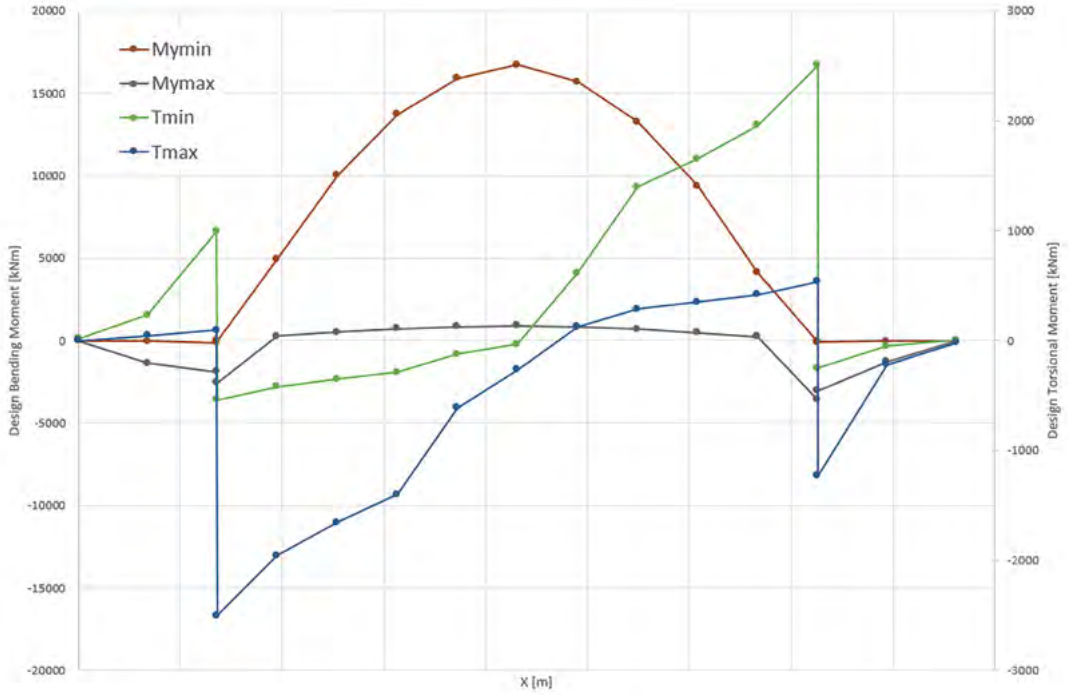

Figure 39. Member forces calculated for box girder after integration of shell stresses.

- The vertical deflection of the concrete box section at final time is only 5 mm, which is negligible (this was also identified in the previous analysis). Thus, the proposed girder cross section shall be considered as stiff enough for deflection control.
- The middle section of the canopy presents vertical deflections double than other sections in front of the piers. This is caused by two main reasons: lack of stiffness of the longitudinal beam which links all stay toes, and lack of stay effectiveness. This last effect is due in turn to two additional factors: lack of piers lateral stiffness, as is shown in deflection elevation, and extreme stay slope which is in the limit of 20°.

For the given canopy span (7.6 m), the maximum calculated deflection represents L/316 (considering L as 2 times the cantilever). This was thought to be a bit excessive (having in mind the objective of L/500) and some improvements to the design were included in the final design:

- The use of shrinkage balanced cement with an adequate expansive additive. This will reduce lightly the maximum compression capacity, but given the low stresses obtained in the calculation it will not represent a significant issue for the design.
- Increase longitudinal beam stiffness (as was observed in the existing steel strengthening) by increasing the section profile up to a HEB260 from the original HEB120.
- Add three additional stays hanging from the box section and controlling the deflection in the middle of the canopy.

With all of three structural improvements, final deflection was controlled up to a maximum value of 19 mm, representing only 40% of the initial estimation with the preliminary solution and L/800. Deflection shows a homogeneous arrangement throughout the length of the structure (figure 38).

Once the structural arrangement adopted was validated through deflection control (main aspect in appearance requirement), member forces were derived in the box girder. For this purpose, the utility *section cut* was used to integrate stresses in shell finite element and calculate relevant member forces to be postprocessed as per code requirements. Member forces distribution for ULS envelopes are plotted in figure 39, obtaining a maximum bending moment of 16 200 kNm, the maximum torsion developed is about 2 500 kNm.

With respect to the stays, the maximum obtained design force was 300 kN, located on the short members linking the box and the canopy slab. This force is easily taken by a MKT bar stay of 42 mm with grade 460, able to support 450 kN each one.

Structurally speaking, in comparison with the original design from 1953, the stays have been distributed throughout the whole canopy, having less capacity. From the original 3∅42 bars (in mild steel quality) isolated stays ∅42 mm of grade 460 have been designed, facilitating the connection detailing to the concrete structure.

4.3. Reconstruction works description

Works started by the demolition of the existing structure. After proper assessment of the existing shoring structure, the old stays were cut, and concrete structure was demolished using a remote-controlled pneumatic hammer. The existing concrete appearance is shown in figure 40, colour and texture indicate that existing concrete was made using high alumina cement as well. After the canopy demolition, piers were also demolished up to the transition level between OPC and aluminous cement, located almost at the existing ground level. All demolitions were carried out in two months.

Figure 40. Existing structure demolition.

Figure 41. Box girder concreting and joint.

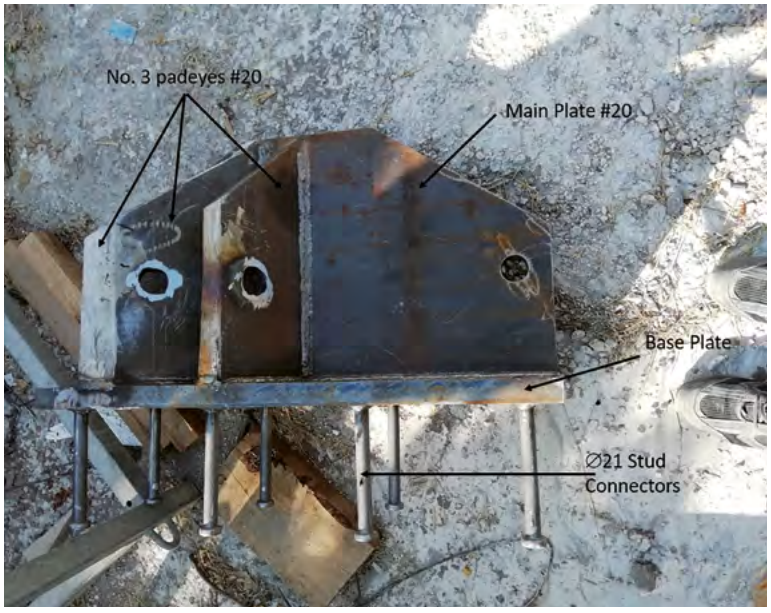

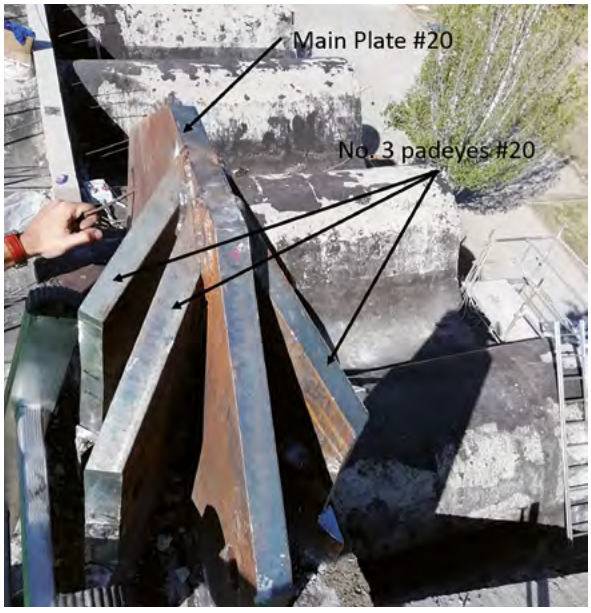

Figure 42. Connection piece details.

Figure 43. view of concrete box girder and piers after piers concreting.

Figure 44. Final appearance of structure and pier top from north façade.

The steel structure used for shoring was updated adding tertiary members to the existing members and providing additional formwork wood plank for the new concrete.

Works started by updating the existing steel shoring to be used for future formwork. Some additional secondary members were added, but in general the structure (and its foundation) was valid for the new structure. The box concrete section was cast in three phases: bottom slab, walls and top slab. The walls were cast in turn in three additional phases providing two construction joints at span quarters (figure 41).

Figure 45. Final appearance of canopy structure.

Figure 46. Door detailing.

Figure 47. Masonry front wall appearance after plaster removal.

Figure 48. South masonry façade detail between different structural modules.

Figure 49. Embedded concrete stiffener and spalled bricks due to corrosion.

Figure 50. Glass fibre reinforcing for brick walls.

Figure 51. Final appearance of brick walls after rehabilitation.

The connection between pier top and the stays was designed with a steel transition piece anchored to the concrete with the aid of eight ∅21 studs. The transition piece is composed by a baseplate, a vertical main plate and three additional padeyes, all welded together to the vertical plate (figure 42). This piece was concreted together with the top part of the pier (figure 43). The stays are anchored to the connection piece by means of a cast iron shackle and pin. Once the stays were positioned, the connection piece was covered with fairing steel plates to maintain the original rectangular shape of the pier top. Waterproofing and protective coatings were added as finalising treatment to the structure. The whole procedure was carried out in four months once the demolition phase was finalised. Figures 44 to 46 shows the final aspect of the canopy once the shoring was removed.

5. MASONRY REHABILITATION

Although the main structural works were focused on the shell roof and entry canopy, rehabilitation of existing brick masonry merits some words in this article. The original state presented a coloured coated plaster, which the owner wanted to remove, restoring the original condition of these elements. After intensive sandblasting, the removal of plaster revealed the existence of severe wall cracking, caused mainly by ground settlement, lack of thermal joints and unsolved interaction between different alignments. Figures 47 and 48 show a graphical description of the masonry's real state. Some concrete stiffeners were provided throughout the wall length. Since the existing stiffeners' rebars developed corrosion, expansion products caused

Figure 52. Final appearance of brick walls after rehabilitation.

Figure 53. Glass sheets enclosure and fixation to shell roof.

not only the concrete to spall but also the covering brick pieces, (figure 49).

Masonry structural rehabilitation was implemented using embedded glass fibre rebars (figure 50). These were provided crossing the crack each 5-horizontal joints, located in the brick bed joint and glued with epoxy resin. The crack was restored using a final coating. Final appearance shows nearly no damage in brick walls, restoring their almost their initial aesthetic (figures 51 and 52).

Building enclosure is finished on its top, with glass sheets 10+10 mm, connected to the masonry and shell roof. Connection is detailed through a piece o stainless steel providing a gap of 10 mm on its top, allowing for deformations of the shell roof (figure 53).

Acknowledgment and gratitude[4]

This article is included in a special number of the scientific magazine Hormigón y Acero to the memory of the one who was Director of the editorial committee: Mr. Luis Ortega. I had the honour of working with him during several joint research projects between the Eduardo Torroja Institute and Geocisa. Later, some bridge rehabilitation project joined us, and, finally, we were colleagues in the Structural Analysis chair at the Escuela de Ingenieros de Caminos de Madrid. From him I did not only learn how to approach existing structures, but also how to interact with other colleagues in the profession and even students. To his memory.

References

[1] Eléybox (1953) Recuerdo de la Feria Internacional del Campo. *Cortijos y Palacios* nº 77, Ed. Casto Fernandez – Shaw, nº 77, Pag 32 – 39. Madrid.

[2] de Coca Leicher, J. (2013). (1950 – 75) *El Recinto Ferial de la Casa de Campo de Madrid*, PhD work (in Spanish). ETS Arquitectura de Madrid. UPM.

[3] Official tourism website of Madrid City. https://www.esmadrid.com/informacion-turistica/pabellon-de-convenciones-casa-de-campo?utm_referrer=https%3A%2F%2Fwww.google.com%2F.

[4] Gómez Barrado, S. Calderón Bello, E. Rodríguez Escribano, R.R. (2018) Proyecto de Ejecución de Medidas Correctoras a Realizar en la Marquesina del Pabellón de Convenciones sito en el Recinto Ferial de la Casa de Campo (Madrid).

[5] Roberts, M.M., S. A. M. T. Jaffrey: BRE Information. 15 15/74 (1975).

[6] Instituto de Ciencias de la Construcción Eduardo Torroja (CSIC). (1993) *Jornadas sobre cemento aluminoso*.

[7] Pérez, M. Vázquez, T. Triviño, F. (1983) Study of stabilized phases in high alumina cement mortars. *Cement and Concrete Research*. Vol. 13, pp. 759-770.

[8] CEN (2007) EN 13791: 2007. Assessment of concrete compressive strength in structures or in structural elements.

[9] Quintero, F. (1988) *Estructuras Metálicas*. U.D. 1.1. La piza aislada. Flexión. Torsion, Escuela de la Edificación, UNED ISBN: 978-84-86957-64-1.

[10] CEN (2004) EN1992-1-1:2004. Eurocode 2. Design of concrete structures. Part 1-1. General Rules and rules for buildings.

4 This section is written by the first author.